Modeling and Validation of Indentation Depth of Abrasive Grain into Lithium Niobate Wafer by Fixed-Abrasive Lapping

Zhu Nannan, Zhu Yongwei *, Xu Jun, Wang Zhankui, Xu Sheng, Zuo Dunwen*

College of Mechanical and Electrical Engineering, Nanjing University of Aeronautics and Astronautics, Nanjing 210016, P. R. China

(Received 20 May 2015; revised 30 August 2015; accepted 11 September 2015)

Abstract: The prediction of indentation depth of abrasive grain in hydrophilic fixed-abrasive (FA) lapping is crucial for controlling material removal rate and surface quality of the work-piece being machined. By applying the theory of contact mechanics, a theoretical model of the indentation depth of abrasive grain was developed and the relationships between indentation depth and properties of contact pairs and abrasive back-off were studied. Also, the average surface roughness (*Ra*) of lapped wafer was approximately calculated according to the obtained indentation depth. To verify the rationality of the proposed model, a series of lapping experiments on lithium niobate (LN) wafers were carried out, whose average surface roughness *Ra* was measured by atomic force microscope (AFM). The experimental results were coincided with the theoretical predictions, verifying the rationality of the proposed model. It is concluded that the indentation depth of the fixed abrasive was primarily affected by the applied load, wafer micro hardness and pad Young′s modulus and so on. Moreover, the larger the applied load, the more significant the back-off of the abrasive grain. The model established in this paper is helpful to the design of FA pad and its machining parameters, and the prediction of *Ra* as well.

Key words: fixed-abrasive lapping; indentation depth; abrasive back-off; lithium niobate wafer; average surface roughness

CLC number: TN305.1 **Document code**: A **Article ID**: 1005-1120(2017)01-0097-08

Nomenclature

z	Abrasive protrusion height (μm)
V_v	Volume fraction
W	Distance of adjacent abrasive layers (μm)
A_r	Total area of one cell (μm^2)
A_m	Total abrasive area in one cell (μm^2)
V_a	Total volume of added abrasives (cm^3)
M_a	Total mass of added abrasives (g)
$\mathbf{V}_r$	Total volume of resin matrix (cm^3)
$\mathbf{M}_r$	Total mass of resin matrix (g)
A_A	Area fraction
L_L	Line fraction
r	Mean radius of abrasive (μm)
N_v	Equivalent abrasive number in simple layer pad (μm · mm^2)
V	Volume of a single particle (μm^3)
N_a	Real number of abrasive protruded on pad surface (μm · mm^2)
N_0	Real abrasive number of protrusion height ranging from h to H (μm · mm^2)
A_0	Nominal contact area between pad and wafer (mm^2)
A'	Nominal area of wafer surface (mm^2)
D	Diameter of abrasive (μm)
h	Mean separation between pad and wafer (μm)
H	The max imum projection height (μm)
d	Abrasive back-off (μm)
a	Semi-width of indentation (μm)
F_0	Normal force on a single abrasive by the deforming wafer (N)
A	Cross-sectional area of single abrasive (μm^2)
H_w	Vickers hardness of wafer surface (HV)
C	Contact stiffness
E^*	Composite modulus (MPa)
A_p	Contact area between abrasive and pad (μm^2)

* Corresponding author: E-mail: meeywzhu@nuaa.edu.cn.

How to cite this article: Zhu Nannan, Zhu Yongwei, Xu Jun, et al. Modeling and validation of indentation depth of abrasive grain into lithium niobate wafer by fixed-abrasive lapping[J]. Trans. Nanjing Univ. Aero. Astro., 2017,34(1):97-104.
http://dx.doi.org/10.16356/j.1005-1120.2017.097.

E_p Young's modulus of pad (GPa)

E_a Young's modulus of abrasive (GPa)

Ra_t Theoretical surface roughness (nm)

Ra_e Experimental surface roughness (nm)

F' Force on a single abrasive by the pad (N)

Greek letters

$\Phi(z)$ Height distribution function of abrasives

ρ_a Density of abrasive (g/cm^3)

ρ_r Density of resin matrix (g/cm^3)

δ Mean indentation depth (nm)

σ_s Yield stress of wafer (MPa)

β Coefficient of contact stiffness

δ_e Elastic-plastic critical deformation (μm)

0 Introduction

As a kind of high efficient ultra-precision machining method, the hydrophilic FA lapping has a good planarization ability and the pad has a unique self-conditioning characteristic through the swelling of its polymer network[1]. Self-conditioning here means that the dulled abrasives drop and fresh ones protrude automatically with the help of the contact force between wafer and pad. In recent years, material properties, manufacturing processing and practical applications of the FA lapping have been investigated. When processing the tungsten blanket wafers, FA pad exhibits an excellent planarization ability[2]. Ra of D2 die steel (AISI standard) after lapping with FA pad can reach 15.1 nm[3]. It is well-known that sapphire removal rate of double-side polishing is highly sensitive to the applied load. Increasing the size of particles fixed in pad can significantly influence the removal rate and surface roughness, and the removal rate can even reach 1 μm/min at most[4]. The hydrolysis of work-piece in FA lapping was studied on CP-4, and the acoustic emission (AE) and coefficient of friction (COF) were collected to analyze its effect on the material removal rate (MRR) and surface quality[5].

Most of researches related to FA lapping focus on its preparation or machining performance evaluation, and few related to the design of FA pad and its machining parameters. In addition, studies on work-piece surface formation and surface roughness in loose abrasive lapping/polishing and grinding process were reported[6-9], while similar ones in FA lapping lapping kept blank.

The purpose of this study is to develop a theoretical model to estimate the indentation depth of abrasive grain into work-piece by utilizing the theory of contact mechanics. Furthermore, based on the obtained indentation depth, the average surface roughness Ra was approximately predicted. The above work is helpful in the design of FA pad and its machining parameters.

1 Modeling of Indentation Depth in FA Lapping

The indentation depth of FA lapping is affected by various factors, such as the real abrasive number, abrasive distribution and protrusion height, the effect of pad matrix property on abrasive "back-off", and abrasives contact mechanics. Follows are the discussion in sequence.

1.1 Real abrasive number N_0

1.1.1 Height distribution function of abrasive protrusion height $\Phi(z)$

To facilitate calculation, the pad surface can be approximated as an ideal plane (Fig. 1). It is assumed that the location of the fixed particles is random, and the distribution function $\varphi(z)$ of abrasive protrusion height is uniformly distributed. Based on the above assumptions, the distribution function of height direction can be expressed as

$$\Phi(z)=\frac{z}{W} \qquad 0<z<W \tag{1}$$

In term of an uniform distribution of spherical abrasives, there would be filled with cells similar to Fig. 1(b) everywhere in arbitrary cross section. Thus, W can be given by

$$W=\sqrt{\frac{\pi r^2}{A_A}}=\sqrt{\frac{\pi r^2}{V_v}} \tag{2}$$

where W is proportional to the particle size and inversely proportional to the square root of V_v.

1.1.2 Real abrasive number N_0

According to the fundamental in quantitative metallography shown in Eq. (3)[10]

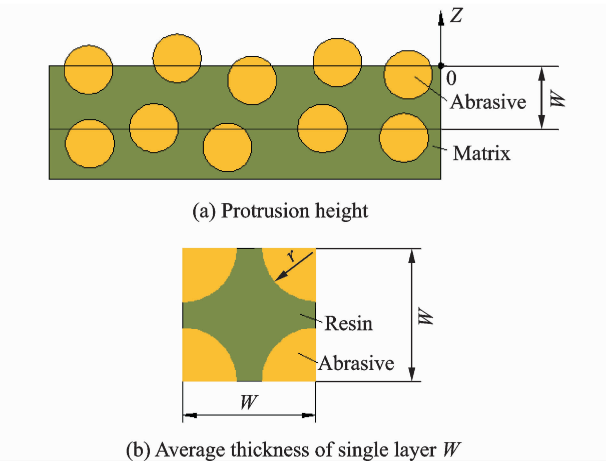

Fig. 1 Schematic illustration of FA pad

$$L_L = A_A = V_v \tag{3}$$

The area fraction A_A is obtained as follow

$$A_A = V_v = \frac{M_a/\rho_a}{M_a/\rho_a + M_r/\rho_r} \tag{4}$$

In term of a uniform distribution of spherical abrasives, the equivalent abrasive number in simple layer pad per unit volume N_v was obtained based on the uniform distribution of abrasives in FA pad, the theoretical number of abrasive protruded on pad surface per unit area N_a is equal to N_v. Abrasives would fall off from resin if its protrusion height exceeds a threshold H. Thus, the range of protrusion height of abrasives is from h to H, then the real abrasive number N_0 can be expressed as

$$N_0 = \int_h^H A_0 N_a \Phi(z)\mathrm{d}z = \int_h^H \frac{A_0 V_v}{\frac{4}{3}\pi r^3}\mathrm{d}z \tag{5}$$

where A_0 is the nominal area of contact between pad and wafer and $A_0 N_a$ the number of abrasives in the contact zone. According to Eq. (5), N_0 is mainly related to V_v and particle size r.

1.2 Indentation depth in FA lapping

The schematic illustration of abrasive grain ploughing in FA lapping is shown in Fig. 2.

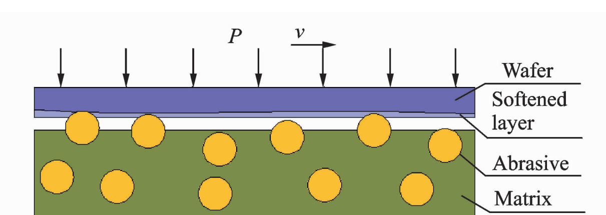

Fig. 2 Schematic of contact between wafer and pad

In this study, it is assumed that the abrasives selected are spherical and rigid. The normal load applied on the wafer P is totally undertaken by abrasives. Typically, diamond is adopted as the abrasive of FA pad. The Young's modulus and hardness of diamond are far greater than those of the pad and wafer. When contacts, only plastic deformation is considered for the wafer, while only elastic deformation for pad resin, especially for those soft pads. It is worth emphasizing that the elastic deformation of soft pad for fine lapping and the phenomenon of abrasive back-off cannot be neglected. According to experience, the abrasives will fall off when abrasive protrusion height exceeds $D/3$[11], which means H is conventionally $D/3$.

1.2.1 Single abrasive contact mechanics and "back-off"

The differences of components and properties between fine lapping pad and rough lapping pad are significant, as shown in Table. 1. The cured resin for rough lapping is much harder than that for fine lapping. The 50 wt% of copper is added into rough lapping pad with a purpose of strengthening resin, increasing the ability to support abrasive grains[12]. Moreover, the fixed particles in rough lapping pad are coated with nickel to improve the bonding strength between particles and resin matrix, and to decrease the abrasive back-off as a result of enlarging the contacting area. Considering the above reasons, the abrasive back-off can be ignored.

Table 1 Components and properties of lapping pads

Component	Fine lapping pad	Rough lapping pad
Matrix	A (soft)	B (hard)
Grit size	W7-14 uncoated Diamond	W14-28 Nickle-coated Diamond
Additive		50 wt% copper
E/GPa	0.6	6

The geometry of contact in each lapping stage is shown in Fig. 3. The black circle in Fig. 3(a) stands for the initial position of abrasive.

The objective of this part is to establish the

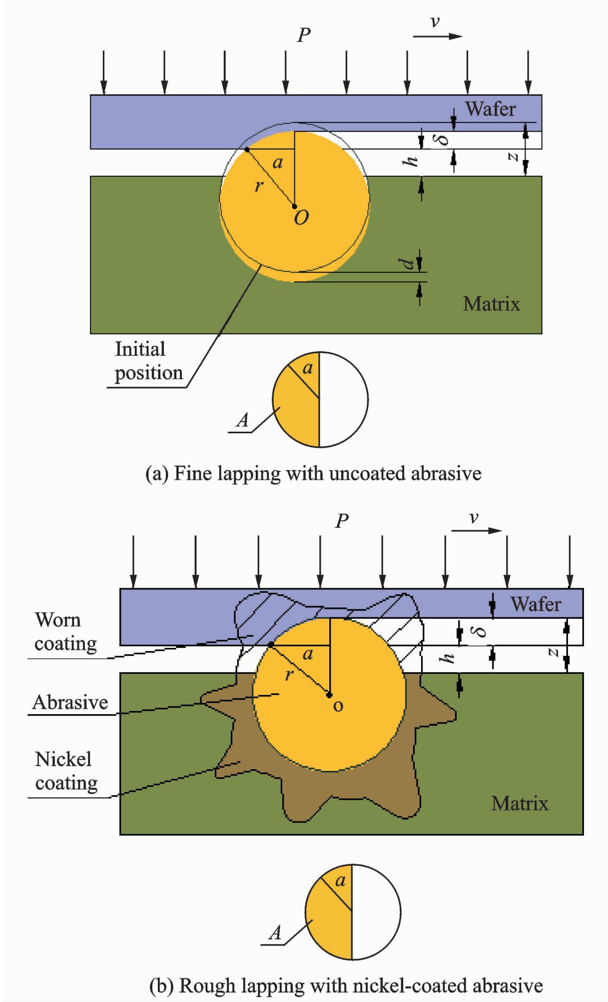

Fig. 3 Geometry of the contact in lapping

relationship between abrasive back-off d and indentation depth δ.

During FA lapping, the cross-sectional area of a single abrasive A described by the half yellow area is related to semi-width of indentation a

$$A=\frac{1}{2}\pi a^2 \tag{6}$$

When δ is small enough[13], we have

$$a^2=\delta D \tag{7}$$

Substituting Eq. (7) into Eq. (6), A would be expressed as

$$A=\pi\delta r \tag{8}$$

Assuming plastic deformation appears on wafer, the normal force on an abrasive F_0 can be calculated by

$$F_0=\sigma_s A=\sigma_s\cdot\pi\delta r \tag{9}$$

where σ_s means the yield stress of wafer, and usually σ_s is 10.58 times as much as the Vickers hardness of wafer H_w[14].

The force imposed on an abrasive results in the back-off[13]

$$F'=Cd \tag{10}$$

where the contact stiffness C is affected by the composite modulus E^* and radius r of abrasive grain, defined as [13]

$$C=2E^*\beta\sqrt{\frac{A_p}{\pi}} \tag{11}$$

where A_p is the contact area between abrasive and pad, and β a coefficient closely related to its shape. And β is equal to 1.000 when the contact profile is circular. Here E^* is the contact composite modulus given by[13]

$$\frac{1}{E^*}=\frac{1-\nu_a^2}{E_a}+\frac{1-\nu_p^2}{E_p} \tag{12}$$

In this study, the contribution of abrasive E_a can be neglected since E_a (1 100 GPa) is much greater than E_p. For most resin polymers, ν_p is around 0.4, then E^* can be written as

$$E^*=1.2E_p \tag{13}$$

Substituting β=1.0 into Eq. (11), we get

$$C=E^*D \tag{14}$$

Considering a single abrasive

$$\sigma_s\cdot\pi\delta r=E^*Dd \tag{15}$$

There is a linear relationship between d and δ. Rearranging Eq. (15) can obtain

$$d=\frac{\sigma_s\pi\delta}{2E^*} \tag{16}$$

As indicated in Fig. 3(a), z, h, d and δ should be satisfied with Eq. (17).

$$z=h+\delta+d \tag{17}$$

Combining Eq. (16) with Eq. (17), the direct variables related to surface roughness δ can be expressed as

$$\delta=\frac{2E^*(z-h)}{\sigma_s\pi+2E^*} \tag{18}$$

1.2.2 Multi-abrasives contact mechanics and average indentation depth

Fig. 2 indicates that as the load is applied on wafer, large quantities of abrasives contact wafer surface and penetrate into them, with an abrasive protrusion height ranging from h to H. The total normal force on contact abrasives F_e can be written as

$$F_e=\int_h^H\sigma_s N_0\pi r\delta\,\mathrm{d}z=\int_h^H\sigma_s\frac{A_0V_v}{\frac{4}{3}r^2}\frac{2E^*(z-h)}{\sigma_s\pi+2E^*}\mathrm{d}z \tag{19}$$

The total normal force on wafer surface F is easily calculated as

$$F = PA' \tag{20}$$

where A' is the nominal area of wafer surface, P the average load, and F_e equal to F.

$$PA' = \int_h^H \sigma_s \frac{V_v A_0}{\frac{4}{3} r^2} \frac{2E^*}{\sigma_s \pi + 2E^*} (z-h) \mathrm{d}z \tag{21}$$

Considering the FA pad pattern, contact asperities are 4/9 of the total area. Substituting $A_0 = 4A'/9$[15] into Eq. (21), it can be simplified as

$$P = \frac{4}{9} \int_h^H \sigma_s \frac{3V_v}{4r^2} \frac{2E^*}{\sigma_s \pi + 2E^*} (z-h) \mathrm{d}z \tag{22}$$

For rough lapping without considering abrasive back-off, there can be seen that

$$P = \frac{4}{9} \int_h^H \sigma_s \frac{3V_v}{4r^2} (z-h) \mathrm{d}z \tag{23}$$

This simplification reveals that the result of δ has nothing to do with the size of wafer. There is only one unknown variable h in Eqs. (22,23) if an FA pad is chosen, since H is assumed as $D/3$. Other variables δ and d can be also calculated after h has been figured out.

2 Experiments

2.1 Verification method and prediction of average surface roughness *Ra*

Small lapping debris within several nanometers and plenty of agglomerates increase the measurement difficulty of debris size simultaneously. Thus, an approximate Ra estimation is adopted from Eq. (24), taking no account of overlap factor[9]

$$Ra = 0.396\delta \tag{24}$$

The rationality of developed model could be verified by comparing the experimental Ra with the model prediction one. From the above model, Ra depends essentially on indentation depth δ. While indentation depth is mainly affected by the size and number of abrasives, the mechanical properties of wafer and pad (the composite modulus of the wafer and pad E^*, contact stiffness C, wafer surface hardness H_w, etc.), abrasive properties and lapping conditions (applied load P).

2.2 Lapping experiments

To verify the developed model, a group of lapping tests were conducted, and the lapping setups are shown in Table 2. All lapping tests were conducted on a CP-4 polisher.

An abrasive-free slurry was used in lapping, and 0.2 wt% of OP-10 was added to improve the wettability of slurry to pad. LN wafers (567HV) with a thickness of 0.5 mm and a diameter of 75 mm were chosen as work-piece. Before each experiment, the FA pad was conditioned by oilstone for fresh pad surface. Each test lasted for 10 min, then the sample was cleaned with deionized water in ultrasonic bath. The average surface roughness Ra and topography of wafers were measured by atomic force microscopy (AFM, Dimension Edge, Bruker, Germany).

Table 2 Parameters in lapping tests

Process	Trial No.	Applied load/kPa	Pad property		
			E_p/GPa	V_v/%	ν_p
Fine lapping (W7-14)	1	6.9	0.6	12.5	0.4
	2	10.5			
	3	15.0			
Rough lapping (W14-28)	4	6.9	6		
	5	10.5			
	6	15.0			

3 Results

Table 3 presents the average measured results and Ra values in the rough lapping (tests No.4, No.5 and No.6) increase with the increase of applied load. This reslut contrasts with h calculated by Eq. (23) and is proportional to δ. While Ra tendency in the fine lapping appears more complex. It will be discussed in detail in Section 4. The measured δ and calculated δ are listed, and the comparison results show that the

Table 3 Experimental values measured by AFM

No.	1	2	3	4	5	6
Ra/nm	4.41	3.94	5.18	31.93	38.14	50.45
Measured δ/nm	11.14	9.95	13.08	80.63	96.31	127.40
Calculated δ /nm	8.87	9.48	11.30	70.67	88.67	106.71
Error/%	20.3	4.7	13.6	12.3	7.9	16.2

errors are limited around 20%. The above modeling in Section 1 is effective. The morphology of used lapping pad was shown in Fig. 4. The abrasives whose protrusion height were higher than the protrusion threshold of $D/3$ fell off and left holes on pad surface.

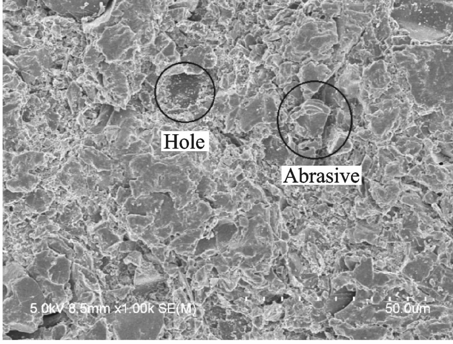

Fig. 4 W7-14 pad surface morphology after lapping

4 Discussion

4.1 Assumption of pad elastic deformation

The elastic-plastic critical deformation δ_e of pad asperities can be related to E^* and H_p, from Eq. (25)[16]

$$\delta_e = \left(\frac{3\pi K_e H_p}{4E^*}\right) R_p \tag{25}$$

where the constant $K_e = 0.4$ and R_p is the simulated radius of asperities on pad surface. When pad asperities are in elastic contact, $d < \delta_e$ should be satisfied. In contrast, the requirement for elastic-plastic contact is obtained as $d > \delta_e$. Substituting H_p and $E^* = 1.2E_p$ into Eq. (25), δ_e can be calculated as

$$\delta_e = 0.08R_p \tag{26}$$

Under this lapping conditions, δ_e is about 0.36 μm substituting fine lapping abrasive′s mean radius 4.5 μm. While d is lower than 200 nm, it can be calculated by Eqs. (16),(24). That is to say, the assumption of pad elastic deformation is reasonable since any d in the fine lapping test is smaller than δ_e.

4.2 Effect of applied load on indentation depth δ and Ra

By the theoretical calculation, the greater the applied load on wafer, the rougher the wafer surface would be (Fig. 5). The experimental results are well consistent with the theoretical ones. As shown in Fig. 5(a), there is a tenuous range that δ decreases with the increasing of the applied load of 10—13 kPa. This phenomenon is consistent with Tian′s research[17]. It is considered that the effective abrasive grain number increases with the applied load to a certain range, along with the abrasive back-off. The synergism of the above two factors results in the decrease of indentation depth.

In this study, with the increase of the applied load P, the abrasive back-off phenomenon becomes more significant.

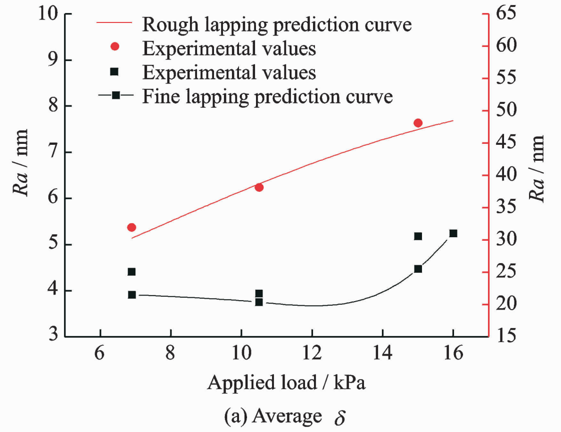

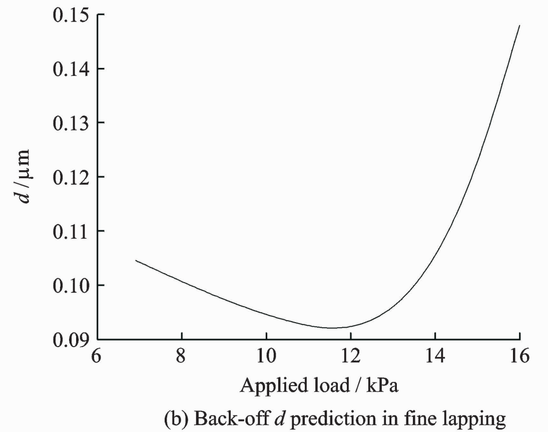

Fig. 5 Effect of applied load on δ and back-off

Fig. 3(a) and Eq. (22) indicate that abrasive original protrusion height is divided into d and δ besides the gap h. Rearranging Eq. (16), the relationship between d and δ can be written as

$$\frac{d}{\delta} = \frac{\pi}{2.4} \cdot \frac{\sigma_s}{E_p} \tag{27}$$

From Eq. (27), the abrasive back-off d is strictly proportional to the indentation depth δ

once material hardness H_w and Young's modulus of pad E_p are determined. When the applied load P increases, the gap h decreases according to Eq. (27), which results in the number of contact abrasives growing rapidly, and the part of d and δ increases simultaneously. This is the mechanism of increasing indentation depth δ and abrasive back-off d.

4.3 Effect of abrasive size on indentation depth δ

Two sizes of commonly used lapping diamond particles were used in this study (Table 1). These two pads used in the tests were embedded with the same mass of abrasives. Thus the number of abrasive grain in the pad with a smaller size is much more by Eq. (5). Each particle bears a little load because of the greater number of contacting particles. The indentation depth on LN crystal surface of fine lapping pad decreased.

5 Conclusions

(1) The surface roughness Ra of soft-brittle crystal LN can achieve several nanometer after FA fine lapping with W14 diamond, applied load of 15 kPa.

(2) Abrasive back-off which appears in FA fine lapping is closely related to the Young's modulus of pad and the yield stress of wafer. Higher applied load and softer pad make the abrasive back-off phenomenon more significant.

(3) The abrasive indentation depth into wafer was significantly affected by applied load, abrasive size and properties of contact pairs. With the increase of the applied load and the particle size, the indentation depth increases.

(4) There is a tenuous range that the δ decreases with the increasing of the applied load of 10—13 kPa in fine lapping because of the increasing abrasive number and the decreasing back-off.

(5) The assumption of pad elastic deformation is reasonable. The theoretical prediction by the developed model is coincided with the experimental results. The developed model could be used to guide the design of FA pad and processing parameters.

Acknowledgements

This work was supported by the Science Foundation of Aviation (No. 2014ZE52055), the National Science Foundation of China (No. 51675276), the Funding of Jiangsu Innovation Program for Graduate Education (No. KYLX_0231), and the Fundamental Research Funds for the Central Universities.

References:

[1] NESPRíAS F, VENTURINO M, DEBRAY M E, et al. Heavy ion beam micromachining on $LiNbO_3$[J]. Nuclear Instruments & Methods in Physics Research, 2009, 267:69-73.

[2] SIVARAJAH P, WERLEY C A, OFORI-OKAI B K, et al. Chemically assisted femtosecond laser machining for applications in $LiNbO_3$ and $LiTaO_3$[J]. Applied Physics A, 2013, 112(3):615-622.

[3] CHOI J Y, JEONG H D. A study on polishing of molds using hydrophilic fixed abrasive pad[J]. International Machine Tools & Manufacture, 2004, 44: 1163-1169.

[4] KIM H, MANIVANNAN R, MOON D J, et al. Evaluation of double sided lapping using a fixed abrasive pad for sapphire substrates[J]. Wear, 2013, 302: 1340-1344.

[5] JU Z L, ZHU Y W, WANG J B, et al. Effect of slurries on chemical mechanical polishing of decorative glasses by fixed-abrasive pad[J]. Optics and Precision Engineering, 2013, 4: 956-962.

[6] FAN C, LIN B, ZHAO J, et al. Modeling and analysis of the material removal profile for free abrasive polishing with sub-aperture pad[J]. Journal of Materials Processing Technology, 2014, 214: 285-294.

[7] BELKHIR N, BOUZID D, HEROLD V. Wear behavior of the abrasive grains used in optical glass polishing[J]. Journal of Materials Processing Technology, 2009, 209(20): 6140-6145.

[8] PARK B, LEE H, PARK K, et al. Pad roughness variation and its effect on material removal profile in ceria-based CMP slurry[J]. Journal of Materials Processing Technology, 2008, 203: 287-292.

[9] AGARWAL S, RAO P V. Modeling and prediction of surface roughness in ceramic grinding[J]. International Journal of Machine Tools & Manufacture, 2010, 50(12):1065-1076.

[10] GEORGE F, VANDER V. Metallography, principles and practice[M]. New York, USA: McGraw-Hill,1984.

[11] ZHU Y W. Analysis of cutting force and the struc-

ture on diamond saw blade[D]. Hunan, China: Central South University, 2002. (in Chinese)

[12] TANG X X, ZHU Y W, WANG C, et al. Realization of self-conditioning process of hydrophilic fixed abrasive pad[J]. Nanotechnology and Precision Engineering, 2014, 12(1):68-73.

[13] POPOV V L, LI Q, LUO J B. Contact mechanics and friction physical principles and applications[M]. Beijing, China: Tsinghua University Press, 2011: 44-48.

[14] YUAN J L. Ultraprecision machining of functional ceramics[M]. Harbin: Harbin Institute of Technology, 2000:45.

[15] LI M, ZHU Y W, YE J F, et al. Removal mechanism in fixed abrasive lapping process[J]. Diamond & Abrasives Engineering, 2010(4):1-6.

[16] SU J X. Study on material removal mechanism of wafer chemical mechanical polishing in IC manufacturing[D]. Liaoning, China: Dalian University of Technology, 2006. (in Chinese)

[17] TIAN C L. The study of lapping mechanism and surface quality on lapping of solid abrasive[D]. Changchun, China: Changchun University of Science and Technology, 2005. (in Chinese)

Ms. **Zhu Nannan** is a Ph. D. candidate of Nanjing University of Aeronautics and Astronautics. She is mainly engaged in soft-brittle material precision ultra-precision processing research.

Prof. **Zhu Yongwei** is the professor and Ph. D. supervisor of Nanjing University of Aeronautics and Astronautics. He received his B. S. degree from Central South University in 1988, M. S. degree from Changsha Research Institute of Mining and Metallurgy in 1991, and Ph. D. degree from Central South University in 2002. His research interests mainly include the preparation and application of nanometer materials, precision ultra-precision machining, and surface engineering research.

Mr. **Xu Jun** is a master candidate of Nanjing University of Aeronautics and Astronautics. He is mainly engaged in the research of fixed-abrasive precision ultra-precision processing.

Mr. **Wang Zhankui** is a Ph. D candidate of Nanjing University of Aeronautics and Astronautics. His research focuses on hard-brittle material precision ultra-precision processing.

Mr. **Xu Sheng** is a master candidate of Nanjing University of Aeronautics and Astronautics. His research mainly focuses on abrasive surface modification research.

Prof. **Zuo Dunwen** is a professor and Ph. D. supervisor of Nanjing University of Aeronautics and Astronautics. His research interests mainly include precision machining, thin film and coating.

(Executive Editor: Zhang Tong)